Chinese Chemical Letters 36 (2025) 110029

Contents lists available at ScienceDirect

Chinese Chemical Letters

journal homepage: www.elsevier.com/locate/cclet

Probing the dynamic properties in the LLPS process *via* site-directed spin labeling-electron paramagnetic resonance (SDSL-EPR) spectroscopy

Ruotong Wei[a,b], Aokun Liu[a,b], Jian Kuang[b], Zhiwen Wang[b], Lu Yu[a,b,*], Changlin Tian[a,b,*]

[a] *High Magnetic Field Laboratory, Hefei Institutes of Physical Science, Chinese Academy of Sciences, Hefei 230031, China*
[b] *Department of Endocrinology, Institute of Endocrine and Metabolic Diseases, The First Affiliated Hospital of USTC, Division of Life Sciences and Medicine, Joint Center for Biological Analytical Chemistry, Anhui Engineering Laboratory of Peptide Drug, Anhui Laboratory of Advanced Photonic Science and Technology, University of Science and Technology of China, Hefei 230026, China*

ARTICLE INFO

Article history:
Received 18 March 2024
Revised 16 May 2024
Accepted 19 May 2024
Available online 19 May 2024

Keywords:
Site-directed spin labeling (SDSL)
Electron paramagnetic resonance (EPR)
Phase separation
Dynamic properties
Molecular tumbling

ABSTRACT

Liquid-liquid phase separation (LLPS) of proteins and nucleic acids is a common phenomenon in cells that underlies the formation of membraneless organelles. Although the macroscopic behavior of biomolecular coacervates has been elucidated by microscopy, the detailed dynamic properties of proteins/peptides during the LLPS process remain poorly characterized. Here, site-directed spin labeling-electron paramagnetic resonance (SDSL-EPR) spectroscopy was employed to characterize the dynamic properties of a minimal model LLPS system consisting of positively charged peptides and RNA. The degree of phase separation, indicated by broadening of the EPR spectrum of the spin-labeled peptide due to slow molecular tumbling, was monitored by EPR. In addition, three distinct populations with varying molecular motion during LLPS, featuring different spectral lineshapes, were identified. These populations included a fast motion component (I), a slower motion component (II) associated with peptides in the dispersed phase and an immobile component (III) observed in the dense phase. With gradual titration of the peptides to RNA, the EPR spectrum gradually shifted, reflecting changes in the populations of the components. Together, SDSL-EPR method not only provides new insights into the dynamic behavior of biomolecules during LLPS, but also offers a sensitive method for biomolecular phase separation processes at the molecular level.

Phase separation is a very common phenomenon in cells and is the basis for the formation of membraneless organelles such as P-bodies and stress granules. Coacervates, as membraneless organelles, have liquid-like characteristics due to the lack of physical membranes, and coacervate droplets can readily exchange biomolecules with their environment and fuse [1,2]. They play an important role in regulating biochemical reactions and improving the adaptability of cells to the environment [3,4]. In addition, many studies have shown that many neurodegenerative diseases, such as Alzheimer's disease and Parkinson's disease, are related to phase-separated proteins [5]. Liquid-liquid phase separation (LLPS) is a phenomenon in which molecules spontaneously demix from the surrounding solvent and condense into a high-concentration phase (dense phase) that is in equilibrium with a dispersed phase that has a lower molecule content. Phase separation is primarily driven by weak interactions, including π-π stacking, cation-π interactions, charge-charge interactions, and transient cross-β-contacts [4]. Many biomolecules can phase separate in cells, the most common of which are proteins and RNA. The ability of proteins to undergo phase separation is associated with their amino acid sequence, with research indicating that proteins undergoing phase separation typically possess intrinsically disordered regions or low-complexity domains, such as the RNA-binding proteins FUS [6], TDP-43 [7], and hnRNPA2 [8] containing low-complexity domains, which support multivalent interactions that aid in phase separation. DNA and RNA have been reported to provide scaffolds for phase separation of proteins or peptides, thereby allowing more complex protein/peptides interactions [9,10].

LLPS is usually characterized *in vitro* by fluorescence microscopy, turbidity measurements [11], and absorption measurements at 280 nm [12]. However, these techniques generate static "snapshots" and cannot provide dynamic information about the molecule as a monomer in coacervates. Solution-state nuclear magnetic resonance (NMR) spectroscopy can be utilized to offer detailed insights into the structure and motion of individual components in coacervates [13–15]. However, the investigation of the

* Corresponding authors.
E-mail addresses: luyuesr@ustc.edu.cn (L. Yu), cltian@ustc.edu.cn (C. Tian).

https://doi.org/10.1016/j.cclet.2024.110029
1001-8417/

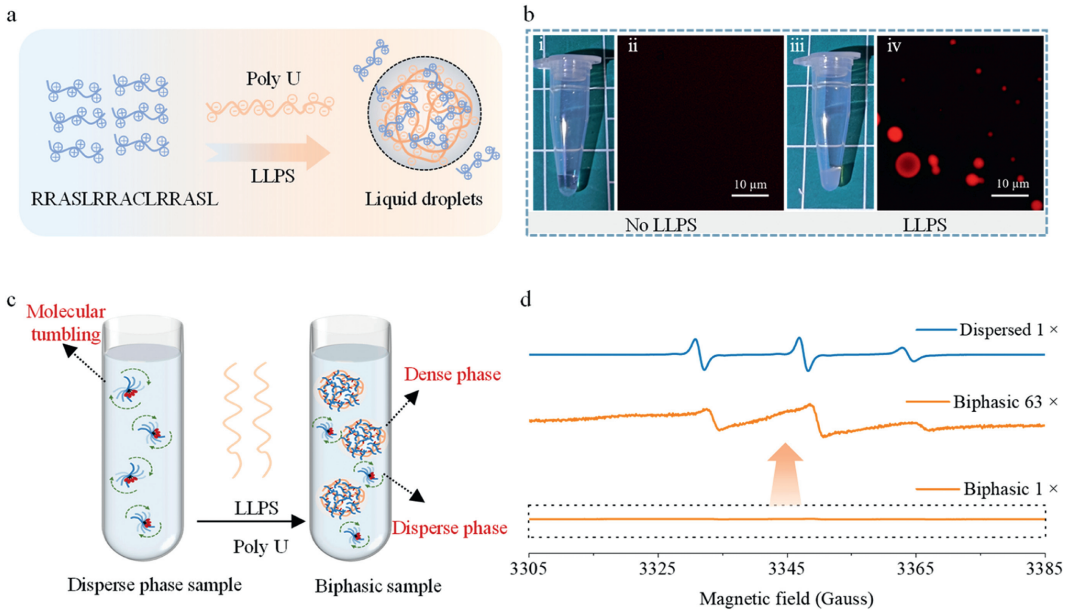

Fig. 1. Arginine-rich peptide phase separation. (a) Schematic illustration of polyU RNA added to a solution of RRASLRRACLRRASL, which results in phase separation. (b) Comparison of the turbidities of the non-LLPS sample (i) and LLPS sample (iii). Fluorescence imaging of the non-LLPS sample (ii) and LLPS sample (iv). Scale bar: 10 μm. The concentration of polypeptides was 1 mmol/L, and that of polyU was 1 mg/mL in the LLPS sample. The concentration of peptides was 1 mmol/L in the non-LLPS sample without polyU. (c) Schematic representation of the transition from the dispersed state to the phase separation state in terms of the molecular dynamic properties. (d) EPR spectra of dispersed (blue line) and biphasic (orange line) samples. The arrow indicates the EPR spectrum of the biphasic sample with 63× magnification. The dispersed sample was incubated in 50 mmol/L HEPES buffer containing 460 μmol/L peptide in the absence of polyU. The biphasic sample was incubated in 50 mmol/L HEPES buffer containing 460 μmol/L peptide in the presence of 1 mg/mL polyU.

condensed phase presents challenges due to the broad line widths resulting from the heightened viscosity and reduced molecular motion within the condense phase. These factors make resonances associated with the condensed phase difficult to detect above the noise, requiring high protein concentrations [16]. Electron paramagnetic resonance (EPR) spectroscopy is a powerful tool for investigation of structure and dynamics of macromolecules in solutions [17]. The size and the dynamic regime of the protein under investigation is not a limit: either globular, membrane, and intrinsically disordered proteins can be studied [18]. In this study, we selected a minimal model of biomolecular condensates: a complex coacervate formed by electrostatic interactions between peptides and RNA. We labeled the peptide with a nitroxide spin label at an engineered cysteine and studied the dynamic properties of the spin-labeled peptide in the dispersed and dense phases using EPR spectroscopy. We demonstrated apparent line broadening in the dense phase due to slow molecular tumbling; therefore, continuous-wave (CW)-EPR spectroscopy is sensitive to phase separation. We also observed three different populations with different molecular motions: peptides in the dense phase exhibiting slow motion, defined as component III, and peptides in the dispersed phase that correspond to fast motion and slower motion, defined as components I and II, respectively. Based on EPR results, we report a hypothetic schematic model for the LLPS of the peptide and RNA.

To gain a deeper understanding of the complex coacervate formed by LLPS of these positively charged arginine-rich proteins and RNA at the molecular level, here, we selected arginine-rich peptides, which contain three RRASL sequences and were previously shown to undergo complex coacervation with RNA, as minimal models of biomolecular condensates [19]. EPR spectroscopy is a powerful tool for measuring local changes in protein dynamics. EPR measurements require a paramagnetic probe, which was introduced *via* site-specific attachment of a methanethiosulfonate spin label (MTSL) to an engineered cysteine; therefore, we designed peptides carrying the desired mutations for spin labeling containing the RRASLRRACLRRASL sequence (Fig. 1a). We started by preparing 1 mmol/L peptide solutions after the addition of polyU, which resulted in phase separation and an opalescent phase-separated solution. We also characterized the phase separation of the peptides by microscopy using carboxytetramethylrhodamine (TAMRA) labeling. In the presence of 1 mg/mL polyU, the peptides formed micrometer-sized droplets. In control experiments which were carried out in the absence of polyU, droplets were not detected by microscopy. Phase separation also led to the fusion of droplets, indicating their liquid-like nature (Fig. 1b). After characterizing the LLPS macroscopic behavior of the peptides by microscopy (Fig. S4 in Supporting information), we explored their dynamic properties using EPR spectroscopy. First, we explored the EPR characteristics of peptides in the dispersed phase state. The CW-EPR spectrum of the peptides before phase separation shows three narrow lines, which indicates fast molecular tumbling and is expected for the disordered structure of the peptides in the dispersed phase state (Figs. 1c and d). Interestingly, the CW-EPR spectrum of the biphasic sample displays dramatically decreased signal intensities and line broadening, potentially a result of attenuated motional narrowing under peptide-RNA and peptide-peptide interactions (Figs. 1c and d). To compare the differences between the spectra of the dispersed phase and biphasic samples, we obtained the spectrum of the biphasic sample at 63× magnification, which revealed the presence of an additional, broader component that was absent in the spectrum of the dispersed sample (Fig. 1d). This component is indicative of a second population of peptide molecules that experience slow molecular tumbling or increased spin-spin interactions consistent with higher peptide concentrations in the dense phase.

To assess the influence of the peptide concentration on the phase separation at a fixed concentration of polyU RNA, we recorded EPR spectra in the peptide concentrations ranging from 10 μmol/L to 1000 μmol/L. The EPR spectra show a concentration dependence. Surprisingly, the spectrum of the 50 μmol/L peptide in the presence of polyU is very different from that of the monomeric native peptide in the absence of polyU and displays

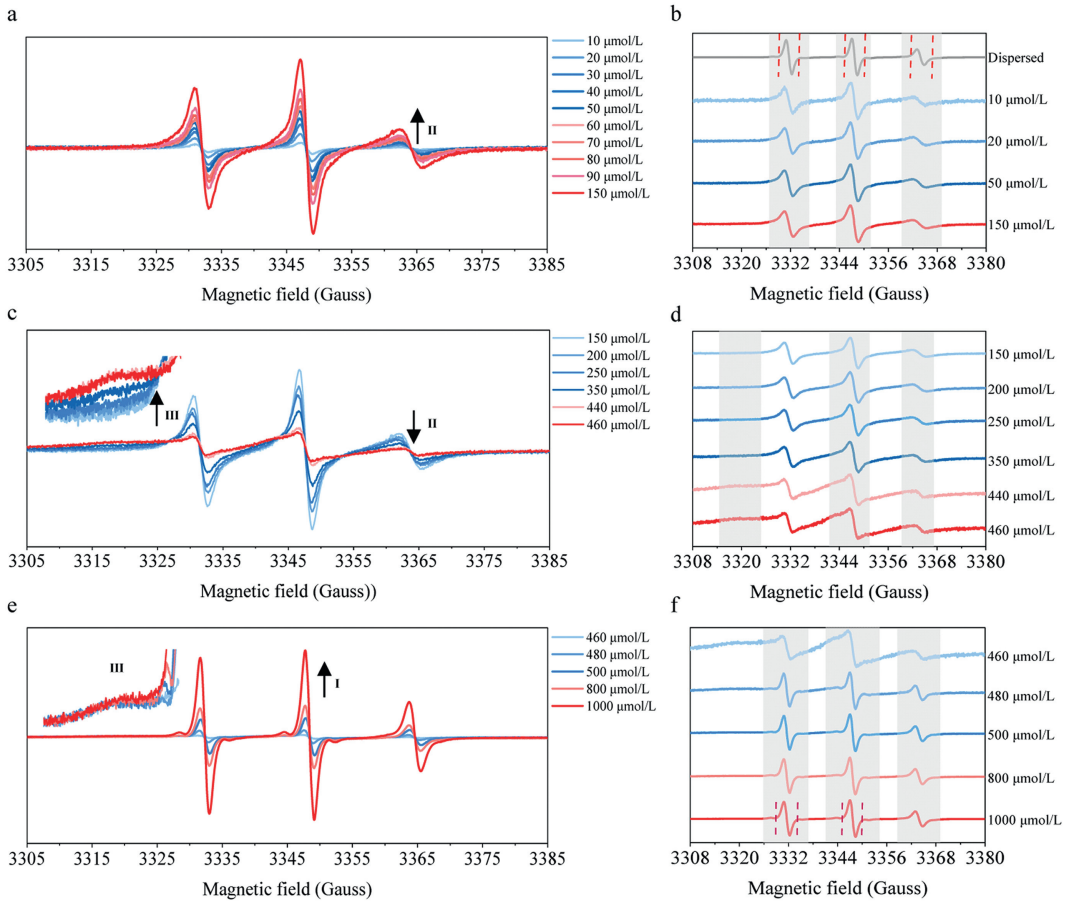

Fig. 2. EPR spectra of the peptide in 50 mmol/L HEPES buffer at different concentrations in the presence of 1 mg/mL polyU. Changes in the signal intensity of the EPR spectra at low, higher, and high peptide concentrations (a, c, and e, respectively). Arrows indicate the signatures in the spectrum of the three different components: a fast motion component (I), a slower motion component (II) and an immobile component (III). The insets show a magnification of the regions marked with arrows. Scaling of the spectra to the same intensity of the central line shown in the monomeric peptide spectrum (gray line) enables clear comparison of EPR spectrum broadening at low, higher, and high peptide concentrations (b, d, and f, respectively).

decreased signal intensities and line broadening (Figs. 2a and b, Fig. S5 in Supporting information). However, we do not observe any liquid droplets at a peptide concentration of 50 μmol/L in the presence of polyU, which is well below the LLPS transition concentration, as shown in Fig. S4 (Supporting information). Here, we assigned component I to dispersed peptides (monomeric native peptides) on the basis of its similar EPR spectrum to that of a highly mobile nitroxide, and we assigned component II to peptides experiencing a slower motion at low concentrations when mixed with polyU. We excluded the possibility that the broadening of the component II spectra was attributed to phase separation since polyU does not induce peptide phase separation at low concentrations. The simplest explanation for the line broadening of component II would be a weak interaction of the peptide with RNA, but this weak interaction is not sufficient to induce phase separation of the peptide at low peptide concentrations; consequently, component II is characterized as binding solely to RNA without entering a phase-separated state, remaining in a dispersed phase state. At low concentrations (*e.g.*, in the 10–150 μmol/L concentration range), the spectra exhibit a clear increase in the spectral signature of component II. At high concentrations (*e.g.*, in the 200–1000 μmol/L concentration range), the spectra exhibit clear features of multiple components, with some indicative of highly restricted motion, exhibiting new signatures and more pronounced broadening than component II; this is, component III (Fig. 2c). Interestingly, the appearance of component III is concomitant with an apparent phase transition, as observed by a white/opaque transition and liquid droplet formation, as shown in Fig. S4 (Supporting information); therefore, the component III spectra display more significant line broadening, potentially as a result of phase separation. LLPS-induced line broadening in EPR spectra was previously observed for several intrinsically disordered proteins [20–22]. The increase in the component III signature with increasing concentration from 200 μmol/L to 460 μmol/L is associated with a decrease in the component II signature (Fig. 2c and Fig. S6 in Supporting information), and the broadening of the spectral lines becomes increasingly obvious, possibly because an increasing number of peptides in component II are transformed into component III with more restricted motion (Fig. 2d). Furthermore, we observed the changes in the EPR spectra at 480–1000 μmol/L peptide concentrations and found that the component III signature signal intensity no longer increased with increasing peptide concentration but stabilized, suggesting that the peptides in the dense phase were largely saturated (Fig. 2e and Fig. S7 in Supporting information). In addition, we also noticed that the EPR spectrum was rather narrow and similar to that of the dispersed phase (monomeric native peptide) (Figs. 2e and f). We speculate that upon reaching saturation in the dense phase, some peptides enter the dispersed phase. The fraction of peptides within the dense phase exhibiting extreme line broadening minimally contributes to the overall signal, leaving only the signals from the dispersed phase.

After establishing the presence of three distinct dynamic components, we proceeded to explore their relationship to LLPS. Here, we present a hypothetic schematic model for the LLPS (Fig. 3a).

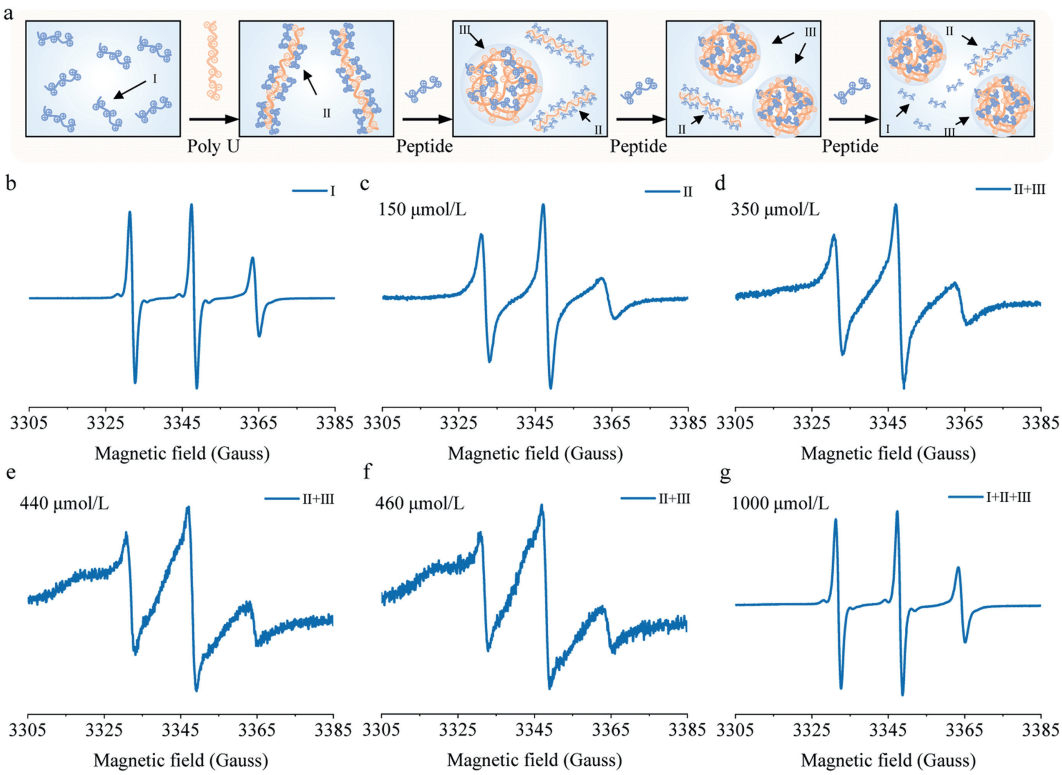

Fig. 3. Hypothetic schematic model for the LLPS of peptides and RNA. (a) Hypothetic schematic illustration of the formation of coacervates between peptides and RNA. (b–g) EPR spectra corresponding to each phase separation stage.

First, the monomeric native peptides as component I are in the dispersed phase, exhibiting fast molecular tumbling, and the EPR spectrum is relatively narrow (Fig. 3b). Subsequently, RNA, a long polyU that carries many negative charges, can bind to arginine-rich peptides and convert peptides into peptide/RNA coacervates by electrostatic interactions. Titration of a smaller amount of peptides into a fixed concentration of RNA does not result in phase separation of the peptides but rather the formation of the oligomer that is only bound to RNA, that is, component II, which is still in the dispersed phase state (Fig. 3c). This shows that component II is a transition form before phase separation. As the peptides are titrated, the newly added peptides occupy the negative charges on the RNA chain, causing component II to transform into component III in the dense phase. A high concentration of peptides in the dense phase leads to spin-spin interactions, resulting in the EPR spectrum of component III being broader than that of component II. Next, component II is consumed, while component III increases, which is consistent with the result that the EPR spectrum gradually broadens (Figs. 3d–f). However, when the peptide concentration reaches 460 μmol/L and component III in the dense phase was saturated, the spectrum shows a clear multicomponent feature, which we believe is due to the fact that there is still a very small amount of component II that will not be consumed and converted into component III, but remains in the dispersed phase. Finally, the newly added peptides enter the dispersed phase and exist in component I form. The total EPR signal of the biphasic sample is a combination of signals from component I, II and III. The signal from component I obscures the broadened signal from component III and the signal from minimal component II, resulting in the appearance of three narrow peaks (Fig. 3g).

Interestingly, low RNA concentrations support the formation of condensates, whereas RNA at a sufficiently high concentration can dissolve reconstituted condensates [23]. For instance, FUS molecules bind to RNA molecule, inducing phase separation, but the highest concentrations of RNA lead to decreased phase separation [13]. We also tested the effect of the polyU RNA concentration on phase separation. The extent of phase separation was slightly affected by a decrease in the polyU concentration from 1 mg/mL to 0.5 mg/mL (Fig. S8 in Supporting information). Titration down to 0.5 mg/mL of RNA resulted in more pronounced broadening of the EPR spectrum of the 400 μmol/L peptide than titration down to 1 mg/mL of RNA, indicating that more peptides entered the dense phase and that the greatest extent of phase separation occurred. Therefore, high RNA concentrations inhibit phase separation.

In this work, EPR spectroscopy was used to provide detailed information on the motion of individual molecule inside coacervates. We demonstrated that EPR is sensitive to phase separation and that the EPR spectrum of spin-labeled peptides in the dense phase exhibited apparent line broadening due to slow molecular tumbling. In addition, EPR was able to detect the entire phase separation process and revealed three components: a fast motion component (I), a slower motion component (II) and an immobile component (III). Peptide phase separation is induced by the polyU. This process does not operate *via* a binary "on/off" mechanism but rather *via* steady advancement. Before phase separation, peptides are not present as monomers but instead exist as oligomers that bind to RNA (II). Component II transition into component III due to an increasing number of peptides binding to a single RNA chain, which initiates phase separation. During phase separation, component II gradually converts into component III until saturation is reached. Following this, the level of component III stays consistent, and surplus peptides are present in a dispersed state. This offers a detailed explanation for the phase separation of biomolecules. Furthermore, we noticed that high RNA concentrations inhibited phase separation.

In summary, we reported the application of SDSL-EPR method in detection and characterization of LLPS processes. Detailed characterization of dynamics properties during LLPS was realized by

analysis of EPR spectral line broadening, which originates from different motional states of spin-labeled molecules during LLPS. This method can be readily applied to the detection and quantitative studies of other LLPS systems. Indeed, we applied SDSL-EPR method in analyzing the LLPS process of a poly-arginine (PolyR)-ATP system, in which the PolyR peptide was spin-labeled and LLPS occurred in the presence of ATP (Fig. S9 in Suppporting information). The successful application of this method within the PolyR-ATP system further demonstrates the excellent applicability of SDSL-EPR approach, which can be widely applied to the analysis of dynamic characteristics during the LLPS process.

Declaration of competing interest

The authors declare that they have no known competing financial interests or personal relationships that could have appeared to influence the work reported in this paper.

CRediT authorship contribution statement

Ruotong Wei: Writing – original draft, Methodology, Formal analysis, Data curation. **Aokun Liu:** Formal analysis, Data curation. **Jian Kuang:** Methodology, Formal analysis, Data curation. **Zhiwen Wang:** Methodology, Formal analysis, Data curation. **Lu Yu:** Writing – review & editing, Project administration, Funding acquisition. **Changlin Tian:** Writing – review & editing, Supervision, Resources, Project administration, Funding acquisition, Conceptualization.

Acknowledgments

This work was supported by the National Natural Science Foundation of China (No. 21927814), the National Key Research and Development Program of China (Nos. 2019YFA0405600, 2019YFA0706900, 2021YFA1200104, 2022YFC3400500), the Strategic Priority Research Program of Chinese Academy of Sciences (Nos. XDB0540200, XDB37040201), Plans for Major Provincial Science & Technology Projects (No. 202303a07020004) and the Youth Innovation Promotion Association, CAS (No. 2022455).

Supplementary materials

Supplementary material associated with this article can be found, in the online version, at doi:10.1016/j.cclet.2024.110029.

References

[1] C.P. Brangwynne, C.R. Eckmann, D.S. Courson, et al., Science 324 (2009) 1729–1732.
[2] A. Molliex, J. Temirov, J. Lee, et al., Cell 163 (2015) 123–133.
[3] T.M. Franzmann, M. Jahnel, A. Pozniakovsky, et al., Science 359 (2018) eaao5654.
[4] E. Gomes, J. Shorter, J. Biol. Chem. 294 (2019) 7115–7127.
[5] S. Alberti, D. Dormann, Annu. Rev. Genet. 53 (2019) 171–194.
[6] A.C. Murthy, G.L. Dignon, Y. Kan, et al., Nat. Struct. Mol. Biol. 26 (2019) 637–648.
[7] D.K. Garg, R. Bhat, Biophys. J. 121 (2022) 2568–2582.
[8] V.H. Ryan, G.L. Dignon, G.H. Zerze, et al., Mol. Cell. 69 (2018) 465–479 e7.
[9] P.R. Banerjee, A.N. Milin, M.M. Moosa, P.L. Onuchic, A.A. Deniz, Angew. Chem. Int. Ed. 56 (2017) 11354–11359.
[10] S. Yao, Y. Liao, R. Pan, et al., Chin. Chem. Lett. 33 (2022) 1545–1549.
[11] Y. Huang, Y. Bai, W. Jin, et al., Biochemistry 60 (2021) 2447–2456.
[12] S. Alberti, A. Gladfelter, T. Mittag, Cell 176 (2019) 419–434.
[13] K.A. Burke, A.M. Janke, C.L. Rhine, N.L. Fawzi, Mol. Cell. 60 (2015) 231–241.
[14] A.E. Conicella, G.H. Zerze, J. Mittal, N.L. Fawzi, Structure 24 (2016) 1537–1549.
[15] S. Guseva, V. Schnapka, W. Adamski, et al., J. Am. Chem. Soc. 145 (2023) 10548–10563.
[16] A.C. Murthy, N.L. Fawzi, J. Biol. Chem. 295 (2020) 2375–2384.
[17] M.R. Fleissner, M.D. Bridges, E.K. Brooks, et al., Proc. Natl. Acad. Sci. U. S. A. 108 (2011) 16241–16246.
[18] F. Torricella, A. Pierro, E. Mileo, V. Belle, A. Bonucci, Biochim. Biophys. Acta, Proteins Proteomics 1869 (2021) 140653.
[19] T. Ukmar-Godec, S. Hutten, M.P. Grieshop, et al., Nat. Commun. 10 (2019) 2909.
[20] W.M. Babinchak, R. Haider, B.K. Dumm, et al., J. Biol. Chem. 294 (2019) 6306–6317.
[21] L. Emmanouilidis, L. Esteban-Hofer, F.F. Damberger, et al., Nat. Chem. Biol. 17 (2021) 608–614.
[22] I. Ritsch, E. Lehmann, L. Emmanouilidis, et al., Angew. Chem. Int. Ed. 61 (2022) e202204311.
[23] C. Roden, A.S. Gladfelter, Nat. Rev. Mol. Cell. Biol. 22 (2021) 183–195.